SUPPORTING INFORMATION

High-Throughput Experimentation for Selective Growth of Small-Diameter Single-Wall Carbon Nanotubes using Ru-Promoted Co Catalysts

Brian M. Everhart,[1] Rahul Rao,[2] Pavel Nikolaev,[2] Tsung-Wei Liu,[3] Diego A. Gómez-Gualdrón,[3] Benji Maruyama,[2] Placidus B. Amama[1*]

[1]Tim Taylor Department of Chemical Engineering, Kansas State University, Manhattan, Kansas 66506
[2]Materials and Manufacturing Directorate, Air Force Research Laboratory, WPAFB, Ohio 45433
[3]Department of Chemical and Biological Engineering, Colorado School of Mines, Golden, Colorado 80401

[*] Corresponding author
P.B. Amama; E-mail: pamama@ksu.edu

Table S1. Average values of the fitting parameters (ν and τ) from Figure 4.

Feedstock-Catalyst Combination	Average ν (Arb. U.)	Average τ (s)	Average T (°C)
Ethylene & Co	34159	9.93	745
Acetylene & Co	51333	7.59	764
Ethylene & Co-Ru	40764	3.49	744
Acetylene & Co-Ru	84764	2.62	754

Table S2: G-band integrated area and small-diameter SWCNT selectivity as functions of temperature for growth on Co and Co-Ru as shown in Figure 3.

Co			Co-Ru		
Temperature (°C)	G-Band Area	Selectivity	Temperature (°C)	G-Band Area	Selectivity
625	71000	0.17	620	122000	0.22
650	162000	0.23	630	136000	0.55
660	320000	0.31	640	178000	0.37
660	203000	0.19	640	55000	0.43
675	298000	0.31	650	215000	0.35
675	253000	0.26	650	203000	0.31
680	330000	0.29	660	134000	0.38
680	336000	0.28	660	210000	0.44
690	263000	0.29	670	210000	0.40
690	427000	0.28	670	120000	0.49
700	263000	0.34	700	165000	0.51
700	352000	0.26	700	140000	0.43
701	409000	0.27	700	202000	0.36
705	431000	0.30	700	138000	0.42
710	445000	0.27	700	251000	0.52
715	585000	0.33	710	318000	0.44
720	322000	0.30	720	150000	0.42
725	495000	0.27	720	158000	0.45
725	442000	0.31	720	146000	0.59
725	510000	0.29	720	147000	0.47
730	400000	0.27	720	164000	0.44
735	701000	0.24	725	306000	0.45
740	525000	0.31	730	159000	0.50
745	809000	0.22	730	159000	0.50
745	774000	0.22	740	159000	0.46
750	402000	0.27	740	240000	0.47
750	788000	0.23	750	180000	0.43
760	467000	0.25	750	240000	0.42
775	770000	0.19	750	318000	0.48
780	495000	0.27	750	280000	0.49
780	490000	0.26	750	228000	0.47
790	626000	0.16	760	147000	0.55
800	626000	0.14	760	147000	0.55
810	467000	0.19	760	266000	0.46
825	452000	0.17	760	266000	0.43
830	416000	0.15	770	198000	0.42
830	485000	0.13	770	353000	0.49
830	293000	0.17	780	138000	0.52
850	386000	0.14	780	138000	0.52
850	362000	0.16	780	131000	0.45
880	254000	0.08	780	277000	0.48
			800	142000	0.51
			800	216000	0.50
			800	228000	0.53
			810	117000	0.33
			810	218000	0.49
			830	140000	0.43
			830	210000	0.57
			840	189000	0.42
			850	282000	0.28
			870	159000	0.28
			920	77000	0.34

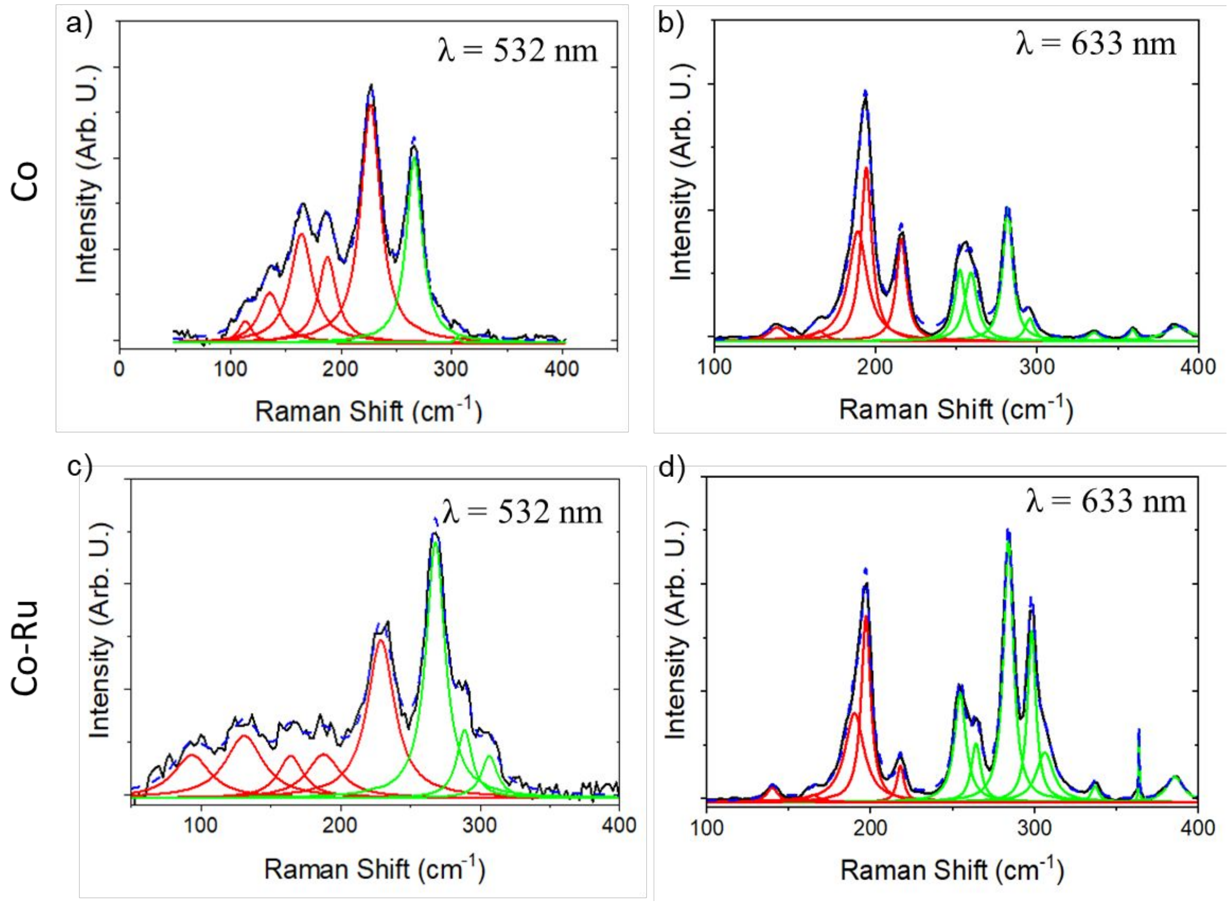

Figures S1. Representative Raman spectra and peak fitting for SWCNTs grown on Co (a) – (b) and Co-Ru (c) – (d) using acetylene as the feedstock. For spectra acquired with 532 nm (a and c) excitation, the small-diameter SWCNT selectivity of Co in (a) is 0.293 (T = 750°), while the selectivity of Co-Ru in (c) is 0.485 (T = 770°). For spectra acquired with 633 nm laser (b and d), the small-diameter SWCNT selectivity of Co in (c) is 0.364 (T = 750°), while the selectivity of Co-Ru in (d) is 0.646 (T = 770°).

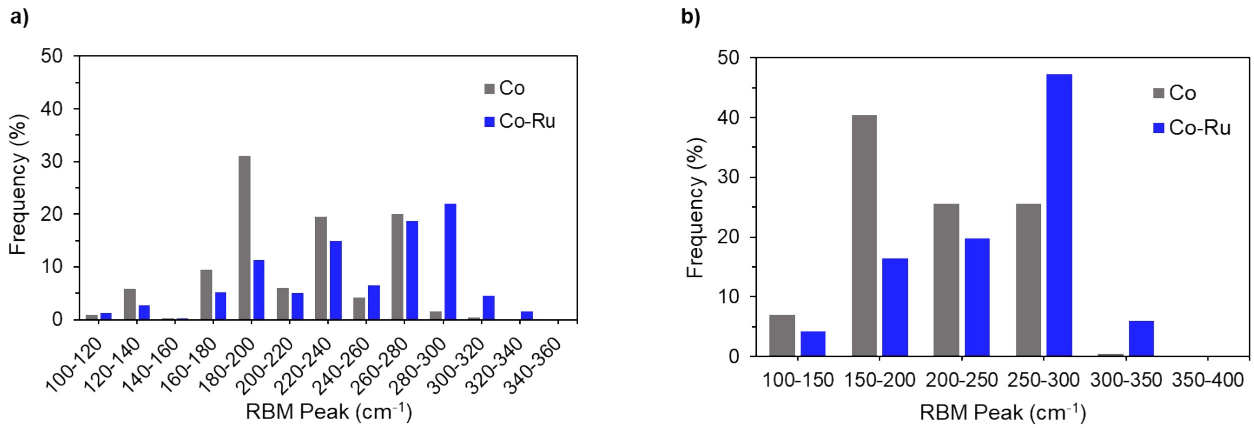

Figures S2. Relative frequency of RBM peaks obtained by averaging Raman data from 532 nm and 633 nm laser excitations shown in Figures 2(e) – (f) versus peak position using 20 cm^{-1} (a) and 50 cm^{-1} (b) brackets.

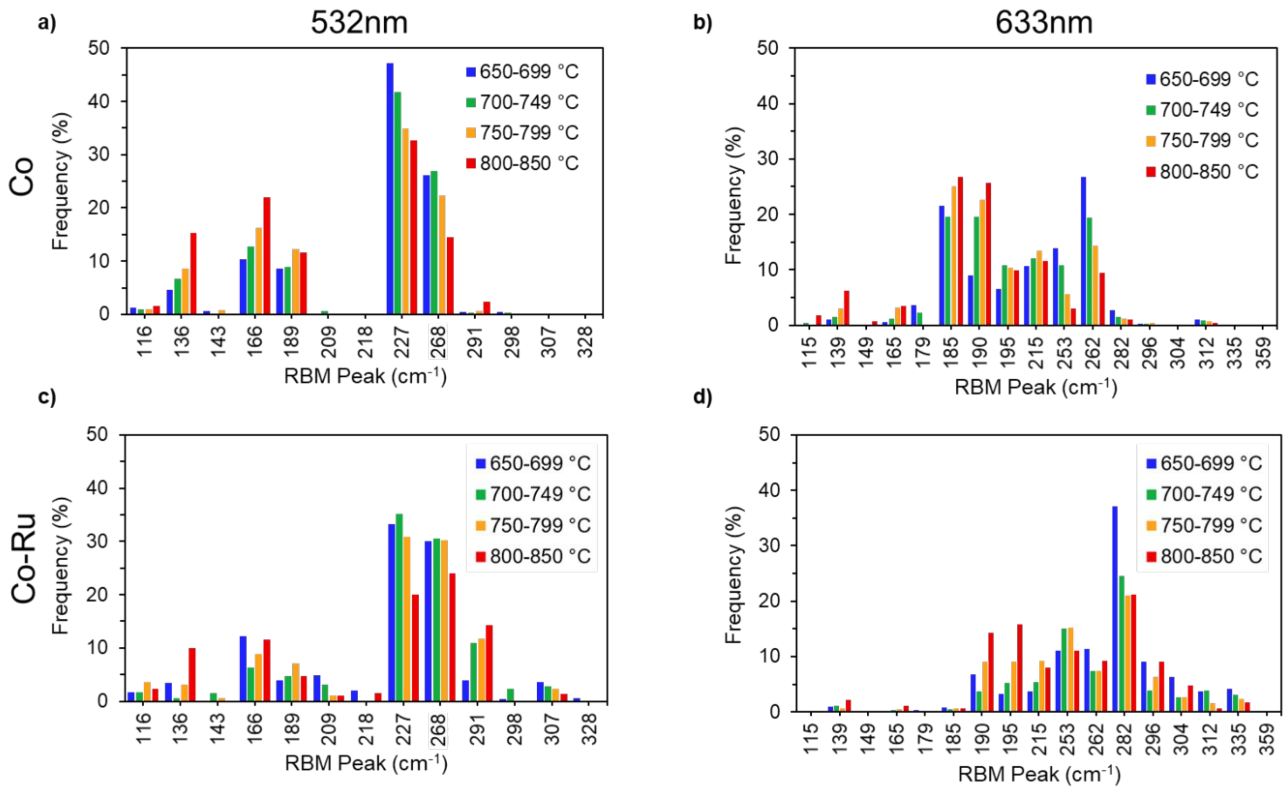

Figures S3. Relative frequency of RBM peaks for Co (a-b) and Co-Ru (c-d) versus peak position using Raman data from 532 nm and 633 nm laser excitations at different growth temperature ranges.

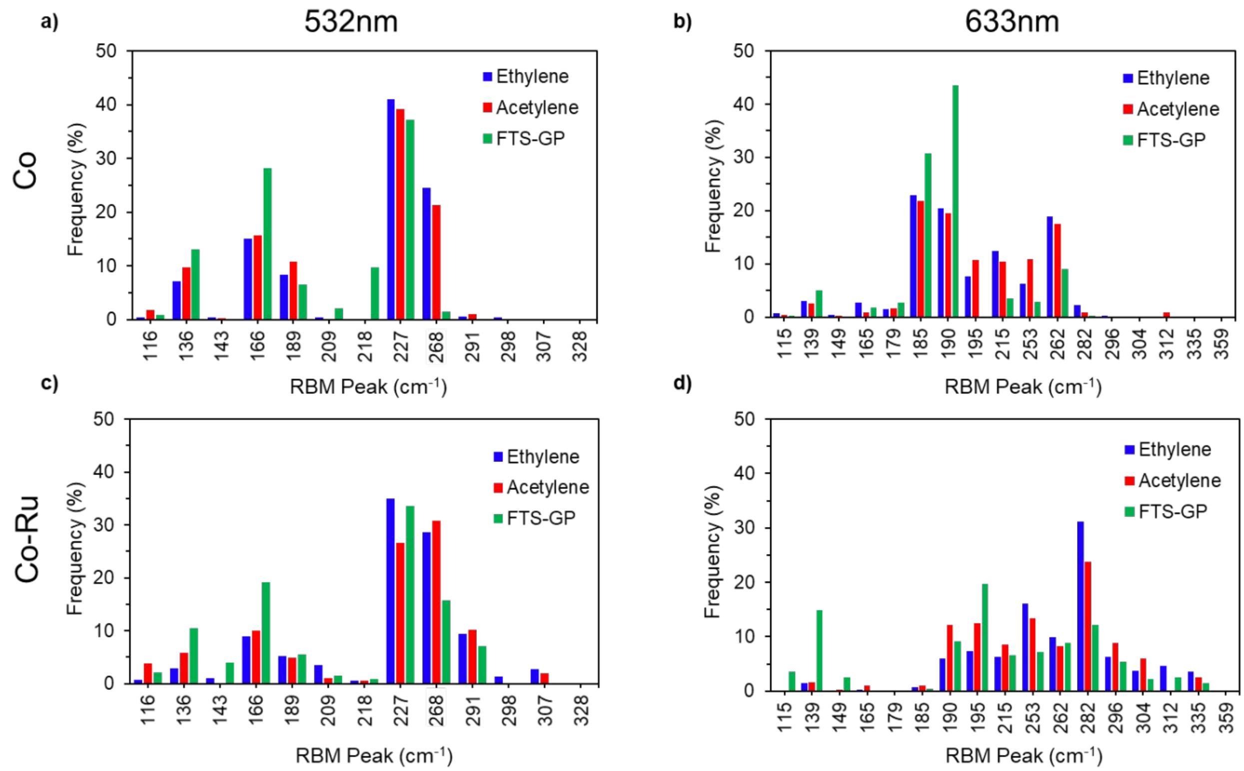

Figures S4. Relative frequency of RBM peaks for growth on Co (a-b) and Co-Ru (c-d) versus peak position using ethylene, acetylene, and FTS-GP precursors. Data are shown for 532 nm and 633 nm laser excitations.

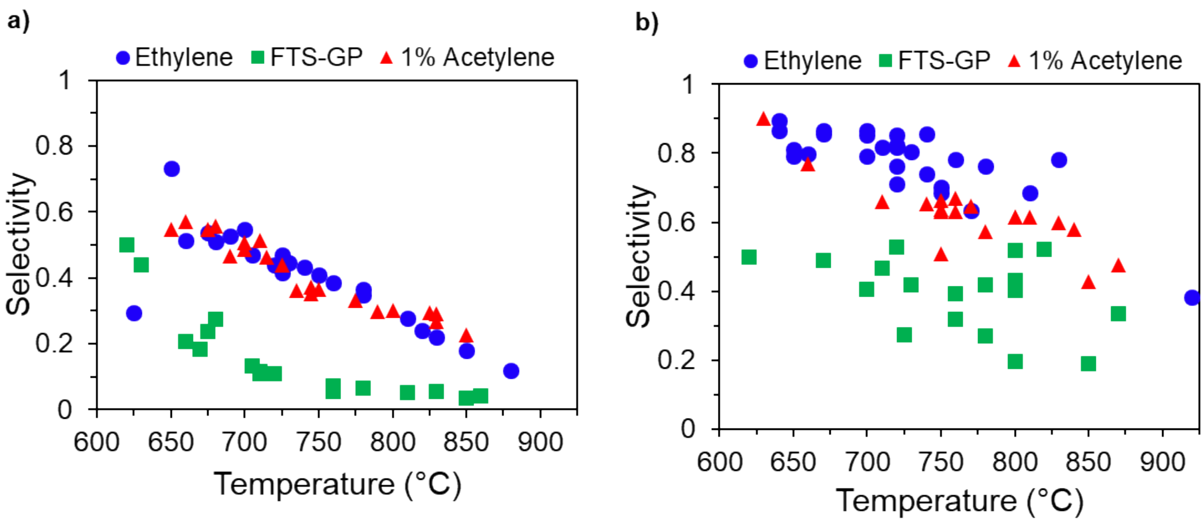

Figures S5. (a) – (b) Difference in selectivity towards small-diameter SWCNTs for the different feedstocks on Co and Co-Ru; data were calculated from Raman spectra acquired with 633 nm laser excitation.

Analysis of C_1 and C_2 values in Equation (1)

$$\omega_{RBM} = \frac{c_1}{d} + c_2 \qquad (1)$$

Values for C_1 and C_2 in Equation 1 have been reported in the ranges of 210 - 260 for C_1 and 0 - 20 for C_2.[1-6] Generally, larger C_2 values correspond to larger interaction effects, such as interaction with dispersion fluid in the case of isolated tubes or tube-tube interactions in bundles.[4, 5, 7] In the case of tube bundling, RBMs can shift as much as 8-12% relative to the RBM frequency of the isolated tube.[6, 8] Kuzmany et al.[6] presented a function for C_2 (using C_1 = 234) that is dependent on both SWCNT diameter and size of SWCNT bundle:

$$C_2 = \frac{c(10.3d - 2.3)2.56}{d}\left(1 - \frac{1}{N^{0.46}}\right) \qquad (2)$$

where c is a scaling factor for tube-tube interaction (listed as 1) and *N* is the number of tubes in the bundle. Considering a SWCNT diameter of 1 nm and for bundles of relatively few tubes, $C_2 \approx 10$, whereas for infinitely large tube bundles, $C_2 = 20.5$. In this work, we have assumed small tube bundles based on the SEM images as evidenced by SEM data; therefore, the average small-diameter SWCNT selectivity has been calculated using $C_1 = 234$ and $C_2 = 10$ (values discussed by Dresselhaus et al.[5]).

Further analysis was carried out to investigate the impact of different values of C_1 and C_2 on the small-diameter SWCNT selectivity for Co and Co-Ru and the results are summarized in Figure S6. Using $C_1 = 214.4$ and $C_2 = 18.7$, as reported for isolated tubes by Telg et al.[2], result in the same selectivity as $C_1 = 234$ and $C_2 = 10$. Assuming very large tube bundles whereby $C_1 = 234$ and $C_2 = 20.5$, the small-diameter SWCNT selectivity decreases slightly; notice that the RBM peak at ~253 cm^{-1} in the spectra obtained with the 633 nm excitation no longer contributes to the selectivity. Small-diameter SWCNT selectivity calculations using $C_1 = 255$ and $C_2 = 20$ are also included in Figure S6 to set a minimum bound, using values at the top end of the ranges presented by Maultzsch et al.[4] Using these values ($C_1 = 255$ and $C_2 = 20$) removes the peak at 262 cm^{-1} in the spectra collected with 633 nm excitation and the peak at 268 cm^{-1} in the spectra collected with 532 nm excitation from the small-diameter SWCNT selectivity.

Results in Figure S6 indicate that the small-diameter SWCNT selectivity on Co-Ru is significantly higher than on Co regardless of the values of C_1 and C_2 chosen. In addition, selectivity is less temperature dependent on Co-Ru compared to Co at all values of C_1 and C_2 examined. Furthermore, as more conservative values for C_1 and C_2 are chosen, the disparity in selectivity increases. For the values $C_1 = 234$ and $C_2 = 10$, the average selectivity of Co-Ru is nearly higher than that of Co by a factor of two. When $C_1 = 255$ and $C_2 = 20$, growth using Co-Ru results in selectivity three times that of Co. It is important to note that while no difference in selectivity is observed between the first and second values of C_1 and C_2, it is likely due to the use of 532 nm and 633 nm laser excitations, which are not in resonance with any RBMs between 233cm^{-1} and 244cm^{-1}.[9] The use of additional laser excitation wavelengths (such as 785nm and 1064nm) would likely result in a small decrease in selectivity between results in the first ($C_1 = 214.4$ and $C_2 = 18.7$) and second ($C_1 = 234$ and $C_2 = 10$) panels.

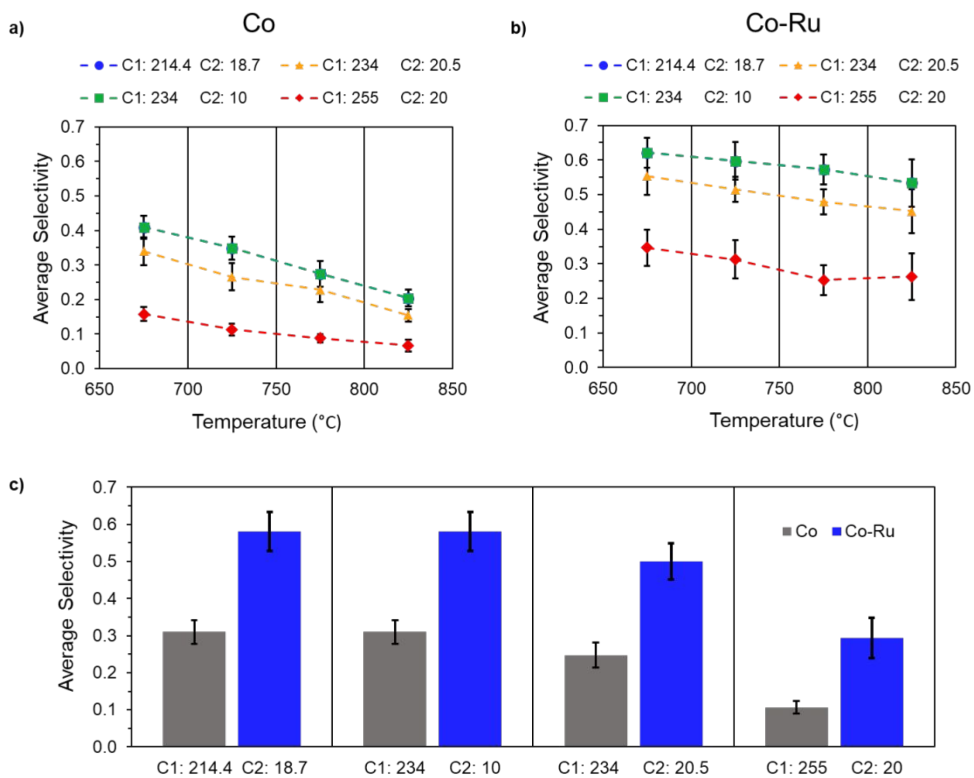

Figures S6. The effect of different C_1 and C_2 values on the average small-diameter selectivity at different growth temperatures for Co (a) and Co-Ru (b). (c) Average selectivity using the four sets of C_1 and C_2 values for Co and Co-Ru.

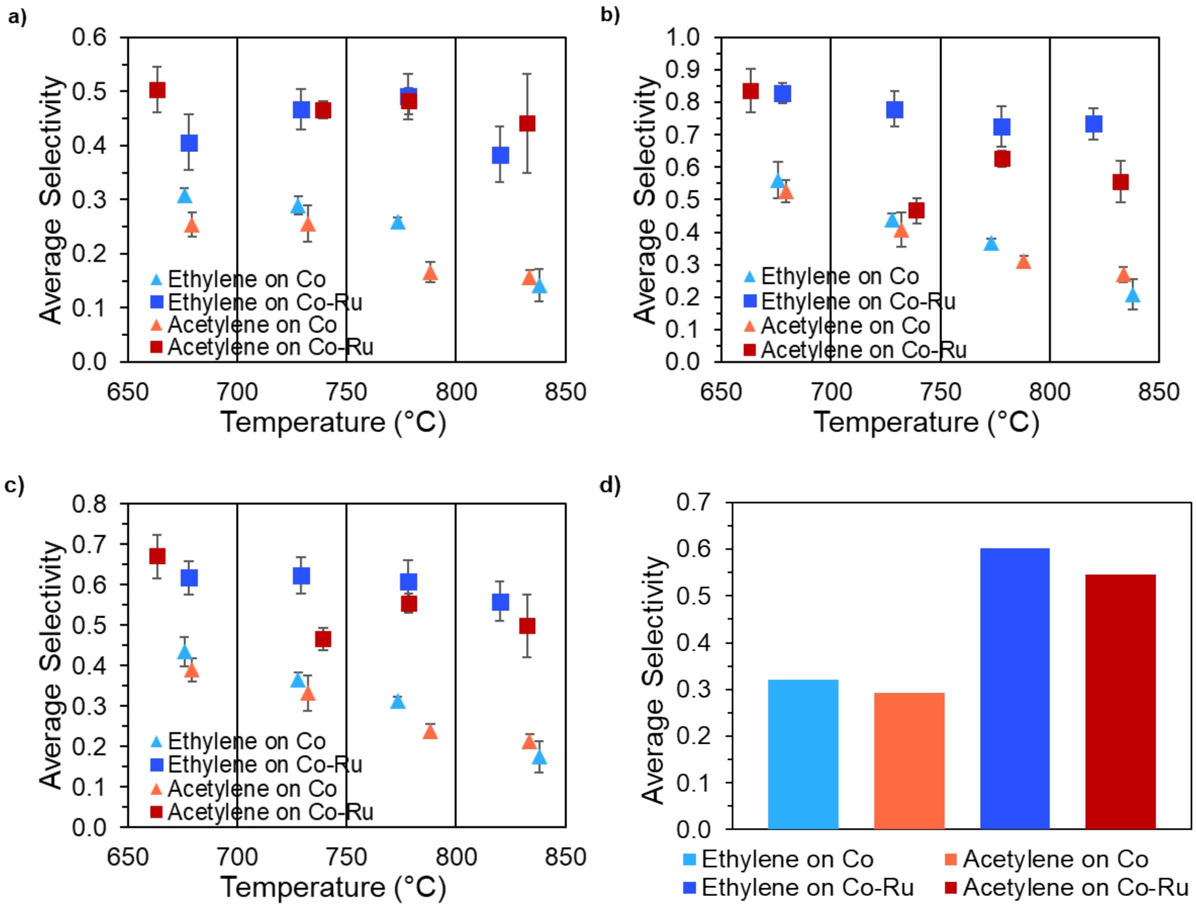

Figures S7. Data used in Figure 3 (c) separated to show small-diameter selectivity for growth performed with ethylene and acetylene as feedstocks: (a) data from 532nm Raman excitation; (b) data from 633nm Raman excitation. (c) Averaged data from spectra acquired using 532nm and 633nm excitation. (d) Histogram of average selectivity across temperature ranges for Co and Co-Ru catalysts. Error bars show standard deviations for the calculated average values.

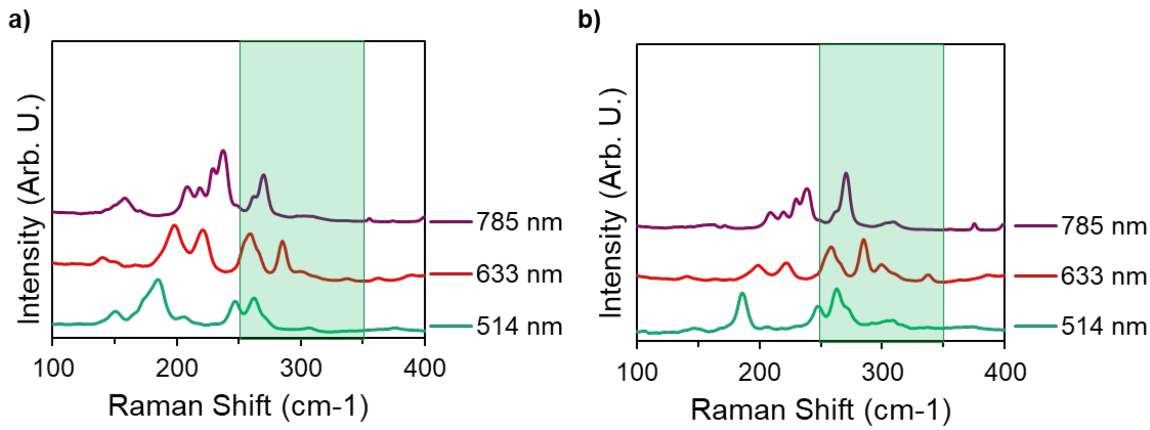

Figures S8. Multi-excitation Raman spectra of SWCNTs grown on Co (a) and Co-Ru (b) catalysts using acetylene as the feedstock; the green shade highlights the small-diameter region (<1 nm).

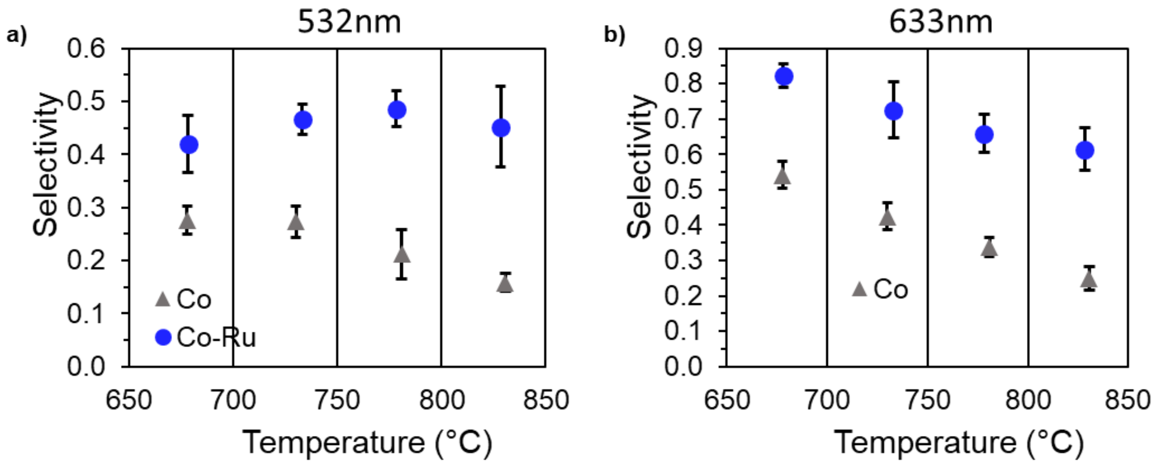

Figures S9. Selectivity data used in Figure 3 (c) separated based on their excitation wavelength: (a) 532 nm, and (b) 633 nm.

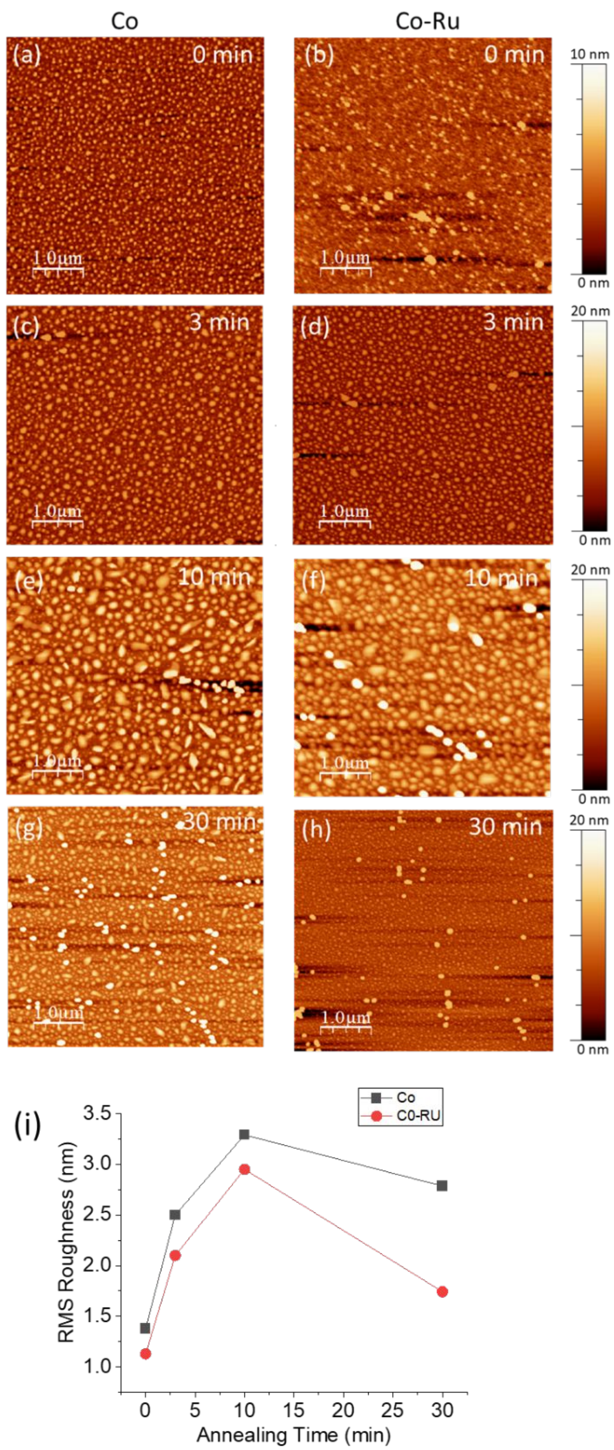

Figure S10. AFM images of as-deposited catalyst films and annealed in H_2/Ar for 0 min (a and b), 3 min (c and d), 10 min (e and f), and 30 min (g and h) for Co (left panel) and Co-Ru (right panel). A plot of RMS roughness obtained from the images as a function of annealing time (i). Films were deposited on Si substrates and annealed in a regular hot-wall CVD.

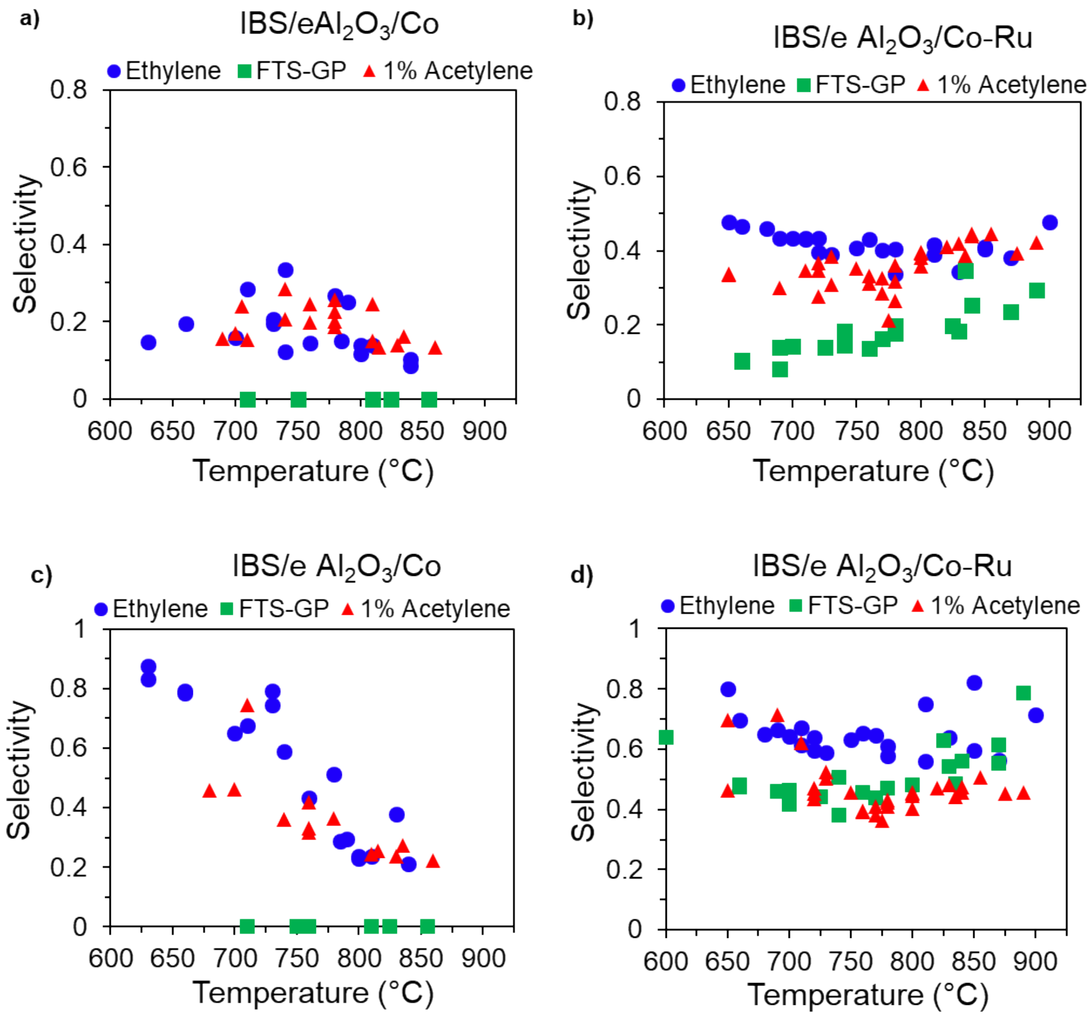

Figures S11. Small-diameter **s**electivity of SWCNTs grown on IBS/e alumina-supported Co and Co-Ru catalysts for the different feedstocks as a function of temperature. (a) – (b) Selectivity calculated from Raman spectra acquired with 532 nm excitation. (c) – (d) Selectivity calculated from Raman spectra acquired with 633 nm excitation.

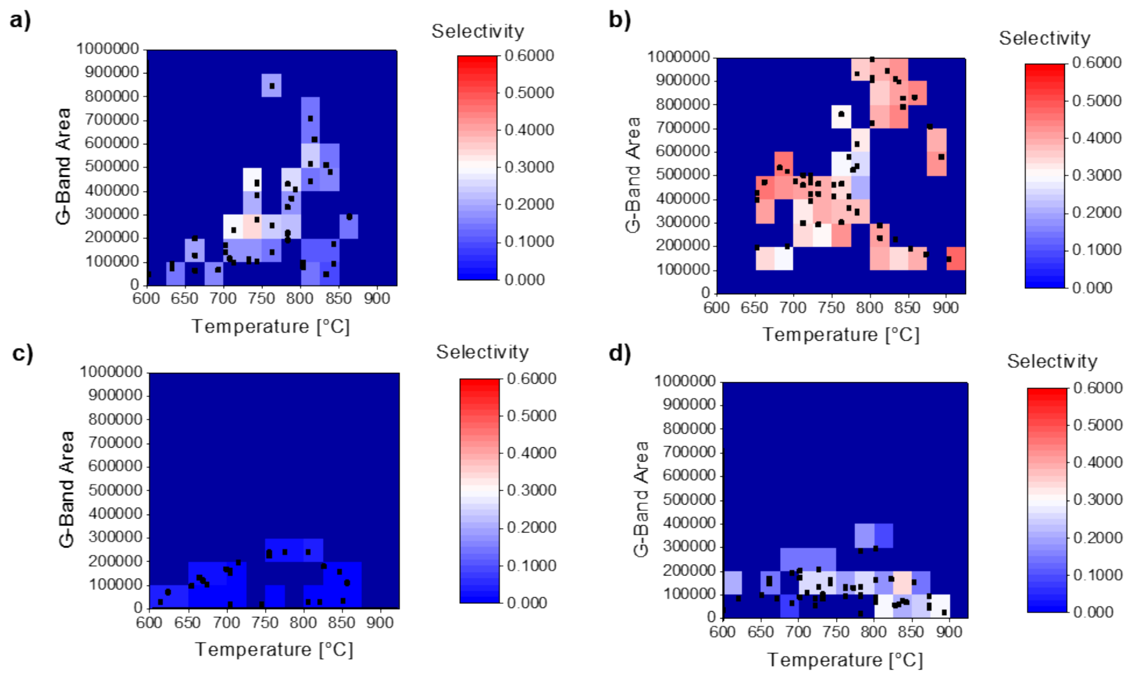

Figure S12. Heat plots illustrating the small-diameter SWCNT selectivity and G-band area (representing abundance of growth) versus temperature for growth on IBS/e alumina-supported Co and Co-Ru catalysts. Plots for growth using ethylene and acetylene on Co (a) and Co-Ru (b). Plots for growth using FTS-GP on Co (c) and Co-Ru (d).

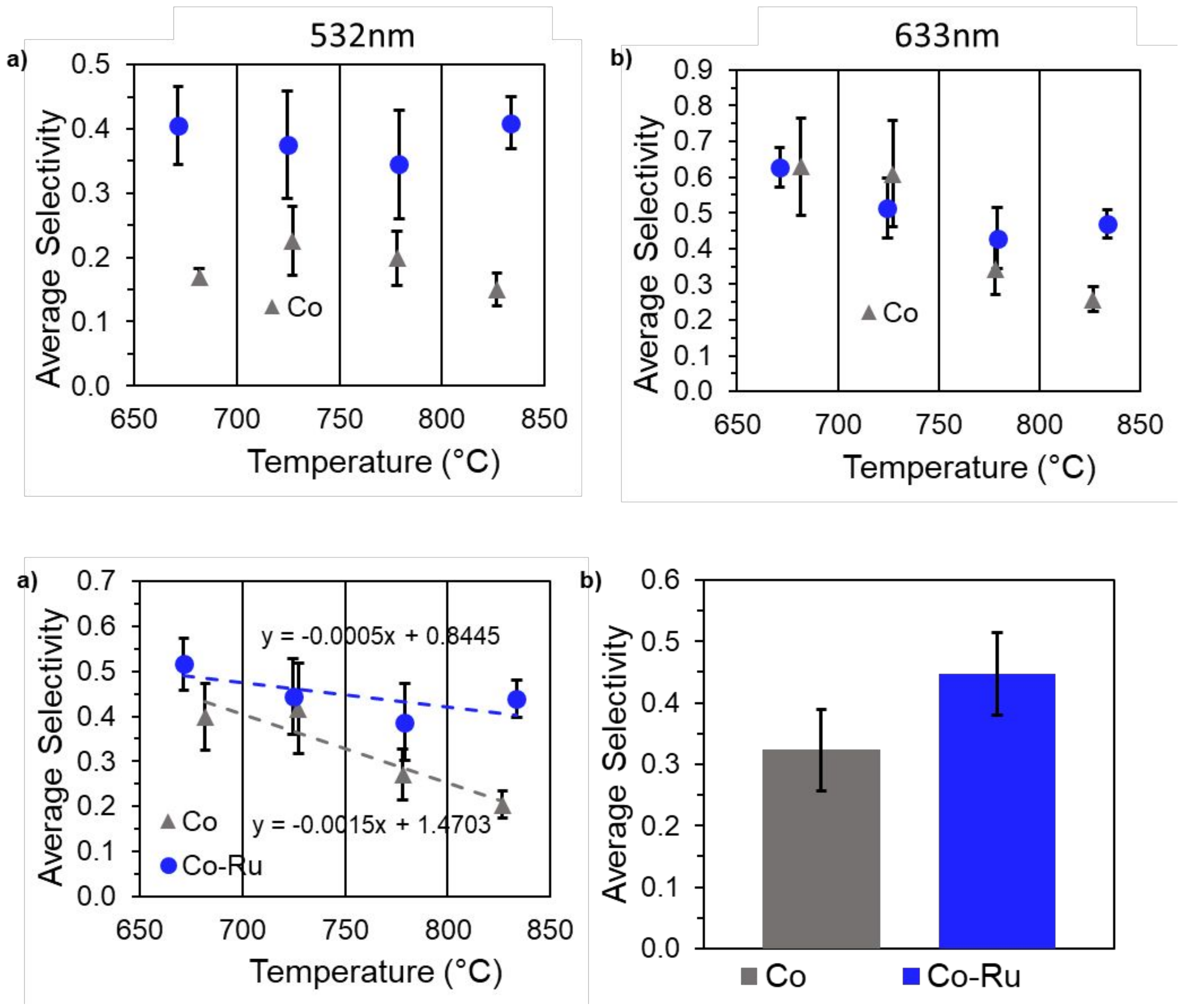

Figure S13. (a) Plots of average selectivity towards small-diameter SWCNTs on IBS/e alumina-supported Co and Co-Ru catalysts versus growth temperature: (a) data acquired with 532nm excitation; (b) data acquired with 633 nm excitation. (c) Average selectivity for combined data acquired with 532 nm and 633 nm excitations. (d) Histogram of average selectivity across temperature ranges for Co and Co-Ru catalysts. Error bars show standard deviations for the calculated average values.

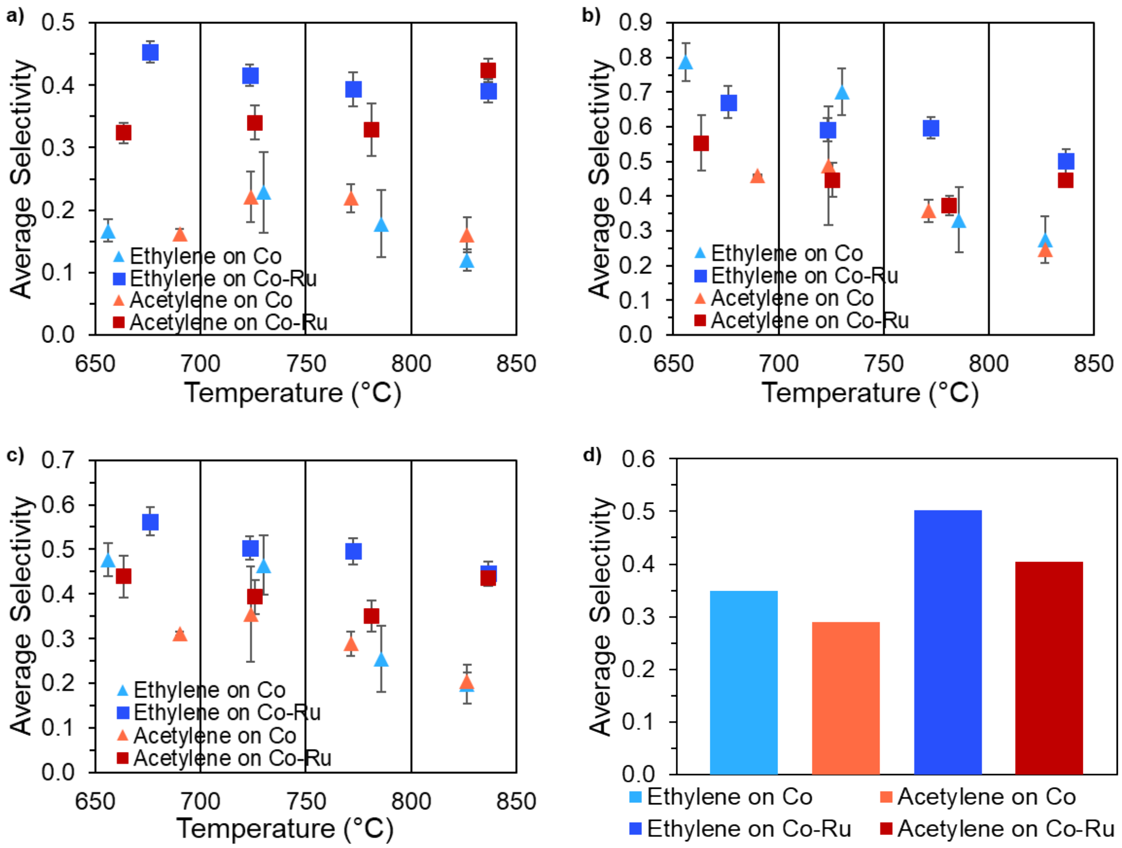

Figures S14. Data adapted from Figure S8 to compare average small-diameter SWCNT selectivity for growth with ethylene and acetylene on Co and Co-Ru catalysts supported on IBS/e alumina: (a) data acquired with 532 nm excitation; (b) data acquired with 633 nm excitation. (c) Average selectivity for combined data acquired with 532 nm and 633 nm excitations. (d) Histogram of average selectivity across temperature ranges for Co and Co-Ru catalysts. Error bars show standard deviations for the calculated average values.

References

1. Jorio, A.; Saito, R.; Hafner, J. H.; Lieber, C. M.; Hunter, M.; McClure, T.; Dresselhaus, G.; Dresselhaus, M. S., Structural (n, m) determination of isolated single-wall carbon nanotubes by resonant Raman scattering. *Phys Rev Lett* **2001,** *86* (6), 1118-21.
2. Telg, H.; Maultzsch, J.; Reich, S.; Hennrich, F.; Thomsen, C., Chirality Distribution and Transition Energies of Carbon Nanotubes. *Physical Review Letters* **2004,** *93* (17), 177401.
3. O'Connell, M. J.; Sivaram, S.; Doorn, S. K., Near-infrared resonance Raman excitation profile studies of single-walled carbon nanotube intertube interactions: A direct comparison of bundled and individually dispersed HiPco nanotubes. *Physical Review B* **2004,** *69* (23), 235415.
4. Maultzsch, J.; Telg, H.; Reich, S.; Thomsen, C., Radial breathing mode of single-walled carbon nanotubes: Optical transition energies and chiral-index assignment. *Physical Review B* **2005,** *72* (20), 205438.
5. Dresselhaus, M. S.; Dresselhaus, G.; Saito, R.; Jorio, A., Raman spectroscopy of carbon nanotubes. *Physics Reports* **2005,** *409* (2), 47-99.
6. Kuzmany, H.; Plank, W.; Hulman, M.; Kramberger, C.; Grüneis, A.; Pichler, T.; Peterlik, H.; Kataura, H.; Achiba, Y., Determination of SWCNT diameters from the Raman response of the radial breathing mode. *The European Physical Journal B - Condensed Matter and Complex Systems* **2001,** *22* (3), 307-320.
7. Milnera, M.; Kürti, J.; Hulman, M.; Kuzmany, H., Periodic Resonance Excitation and Intertube Interaction from Quasicontinuous Distributed Helicities in Single-Wall Carbon Nanotubes. *Physical Review Letters* **2000,** *84* (6), 1324-1327.
8. Henrard, L.; Hernández, E.; Bernier, P.; Rubio, A., van der Waals interaction in nanotube bundles: Consequences on vibrational modes. *Physical Review B* **1999,** *60* (12), R8521-R8524.
9. Kataura, H.; Kumazawa, Y.; Maniwa, Y.; Umezu, I.; Suzuki, S.; Ohtsuka, Y.; Achiba, Y., Optical properties of single-wall carbon nanotubes. *Synthetic Metals* **1999,** *103* (1), 2555-2558.